

Assessing the persistence of the N–H...N hydrogen bonding leading to supramolecular chains in molecules related to the anti-malarial drug, chloroquine

Carlos R. Kaiser,^a Karla C. Pais,^a Marcus V. N. de Souza,^b James L. Wardell,^{c,d} Solange M.S.V. Wardell*^b and Edward R.T. Tiekink*^e

^a *Instituto de Química, Departamento de Química Orgânica, Universidade Federal do Rio de Janeiro, CEP 68534, 21941-972 Rio de Janeiro - RJ, Brazil*

^b *FioCruz – Fundação Oswaldo Cruz, Instituto de Tecnologia em Fármacos – FarManguinhos, Rua Sizenando Nabuco, 100, Manguinhos, 21041-250, Rio de Janeiro, RJ, Brazil. Fax 55.21 2552-0435; Tel: 55 21 2552-0435; E-mail: solangewardell@yahoo.co.uk*

^c *Department of Chemistry, University of Aberdeen, Meston Walk, Old Aberdeen, AB24 3UE, Scotland*

^d *Centro de Desenvolvimento Tecnológico em Saúde (CDTS), Fundação Oswaldo Cruz (FIOCRUZ), Casa Amarela, Campus de Manguinhos, Av. Brasil 4365, 21040-900, Rio de Janeiro, RJ, Brazil*

^e *Department of Chemistry, The University of Texas at San Antonio, One UTSA Circle, San Antonio, Texas 78249-0698, USA. Fax 1 210 458 7428; Tel: 1 210 458 5774; E-mail: Edward.Tiekink@utsa.edu*

Fig. S1 Molecular structure of (1), showing crystallographic numbering scheme and displacement ellipsoids at the 50% probability level. The non-hydrogen atoms of the molecule are essentially co-planar and the amino-hydrogen atom is directed towards the aromatic system. This geometry is repeated in all of the structures described herein, see Figs S2 – S8.

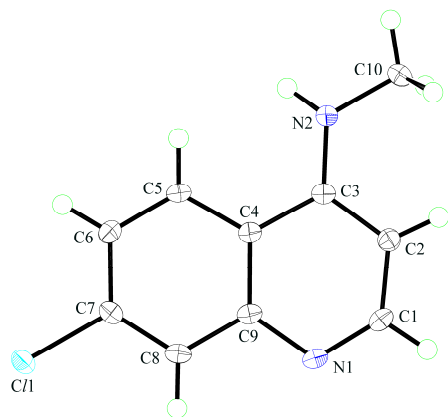


Fig. S2 Molecular structures of (2), showing crystallographic numbering scheme for the two independent molecules and displacement ellipsoids at the 50% probability level. The root mean square fit between bond distances is 0.011 Å and 0.35° for bond angles, indicating a high degree of similarity between the independent molecules. The N2-bound alkyl chain adopts an extended conformation approximately normal to the plane of the fused rings ($C3-N2-C10-C11 = -81.4(3)^\circ$ and $N2-C10-C11-C12 = 177.8(2)^\circ$; $85.4(3)^\circ$ and $179.0(3)^\circ$ for molecule “a”, respectively).

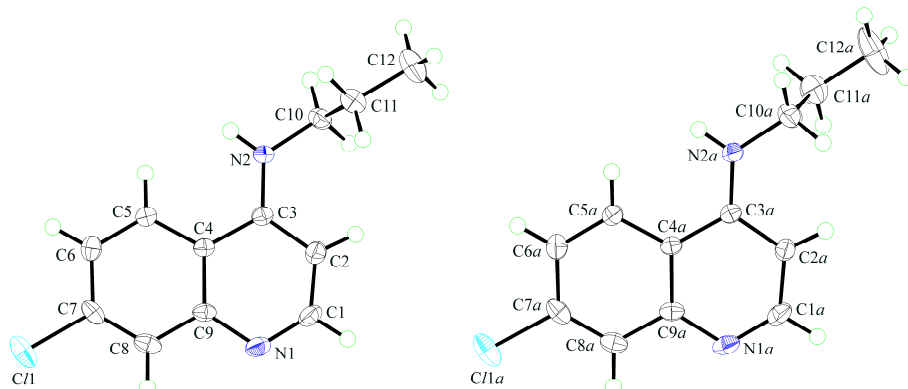


Fig. S3 Molecular structures of (3), showing crystallographic numbering scheme for the two independent molecules and displacement ellipsoids at the 50% probability level. The root mean square fit between bond distances is 0.005 Å and 0.52° for bond angles, indicating a high degree of similarity between the independent molecules. The n-butyl groups, which adopt an extended conformation, are co-planar with the fused ring systems ($C3-N2-C10-C11 = -167.6(2)^\circ$ and $C10-C11-C12-C13 = -174.2(2)^\circ$; $173.1(2)$ and $178.2(2)^\circ$ for molecule “a”, respectively).

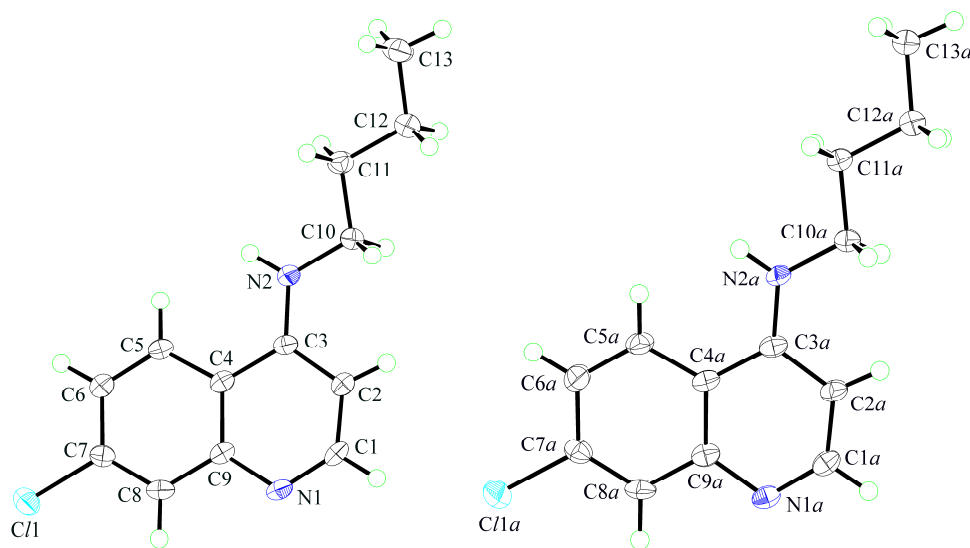


Fig. S4 Molecular structure of (4), showing crystallographic numbering scheme and displacement ellipsoids at the 50% probability level. The N2-bound substituent tends to fold back over the fused ring system as seen in the $C3-N2-C10-C11$ and $N2-C10-C12-C1$ torsion angles of $-77.7(3)$ and $-68.6(3)^\circ$, respectively.

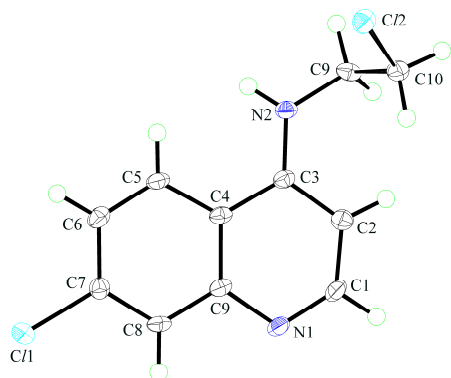


Fig. S5 Molecular structure of (**5**), showing crystallographic numbering scheme and displacement ellipsoids at the 50% probability level. The N2-bound substituent tends to fold back over the fused ring system as seen in the C3-N2-C10-C11 and N2-C10-C12-N3 torsion angles of 79.8(3) and 62.3(3)°, respectively.

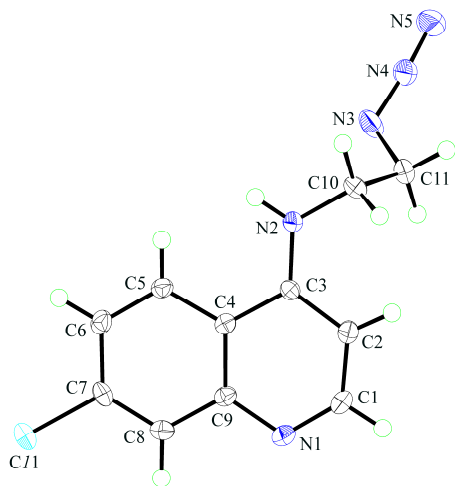


Fig. S6 Views of the crystal packing in (**1**): (a) a layer comprising parallel supramolecular chains, and (b) projection down the *a*-axis emphasising the stacking of layers. Colour code in this and diagrams shown in Figs S7 – S10: chloride, cyan; nitrogen, blue; carbon, grey; and hydrogen, green. For reasons of clarity, only those hydrogen atoms engaged in hydrogen bonding are shown.

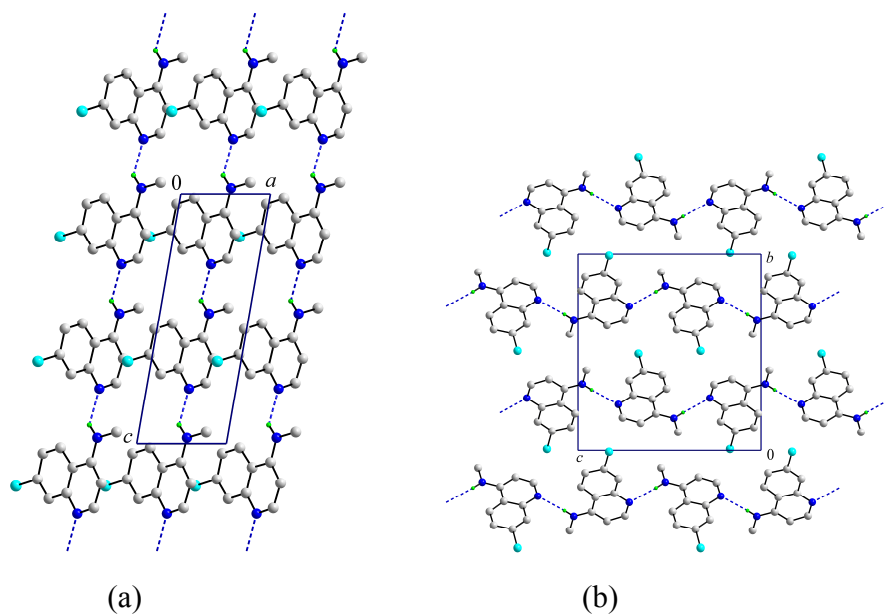


Fig. S7 Views of the crystal packing in (2): (a) a layer comprising anti-parallel supramolecular chains, and (b) projection down the *a*-axis emphasising the stacking of layers.

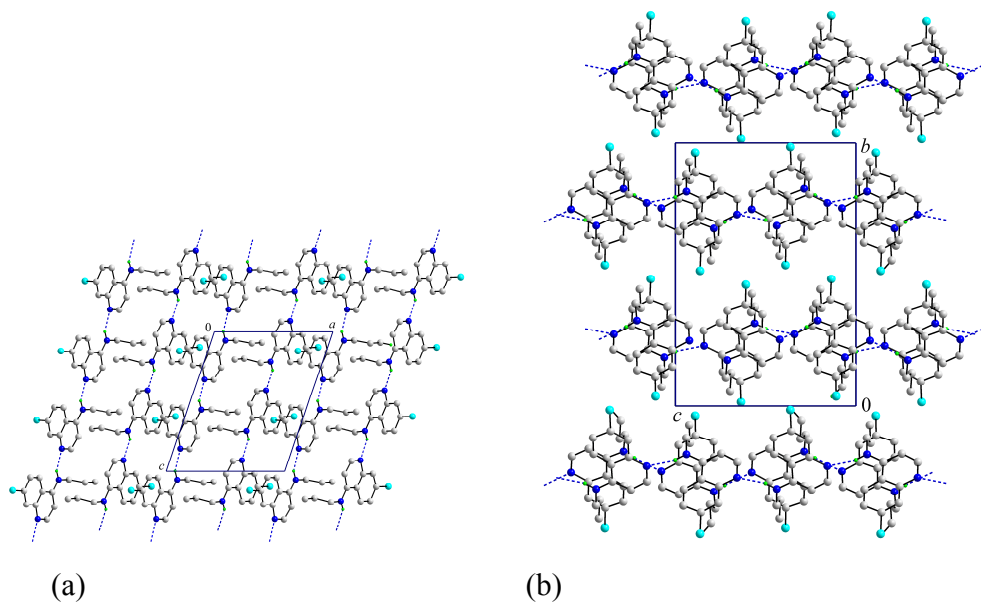


Fig. S8 Views of the crystal packing in (3): (a) a layer comprising anti-parallel supramolecular chains, and (b) projection down the *a*-axis emphasising the stacking of layers.

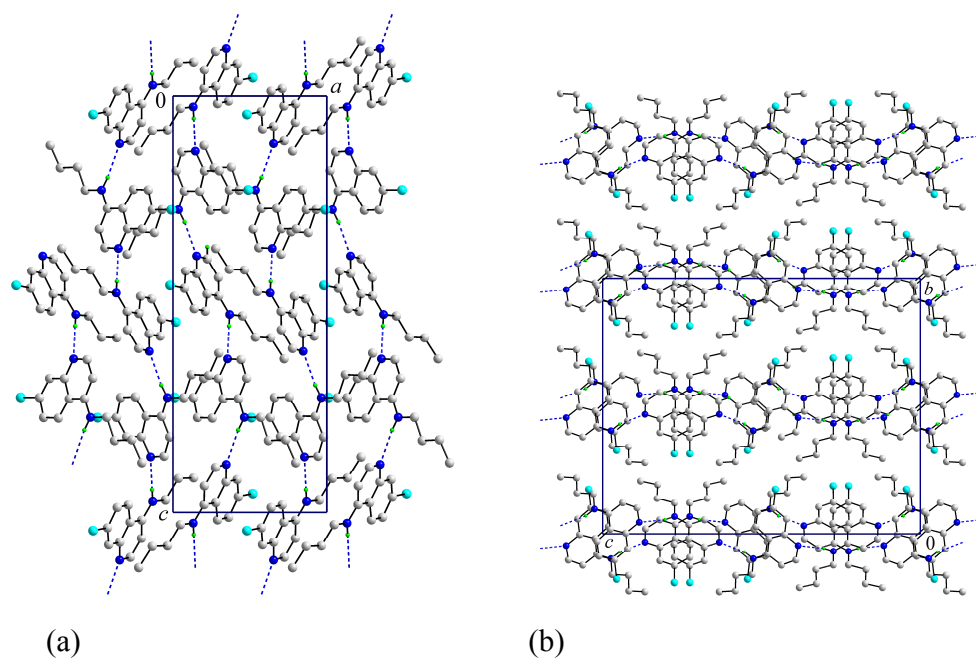


Fig. S9 Views of the crystal packing in (4): (a) a layer comprising parallel supramolecular chains, and (b) projection down the *a*-axis emphasising the stacking of layers.

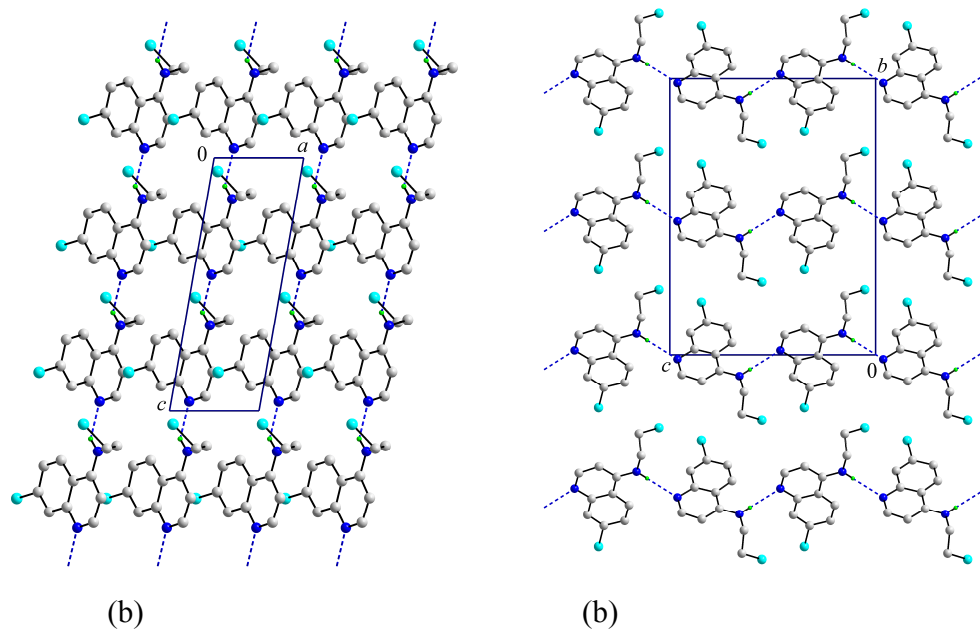


Fig. S10 View of the crystal packing in (5): a layer comprising anti-parallel supramolecular chains.

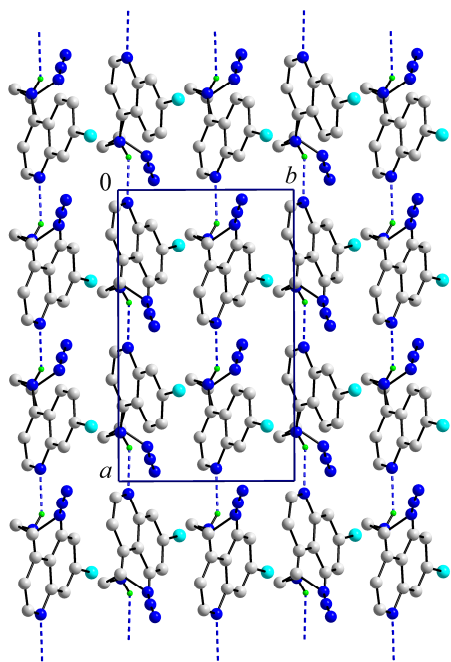


Fig. S11 Molecular structure of (6), showing crystallographic numbering scheme and displacement ellipsoids at the 50% probability level.

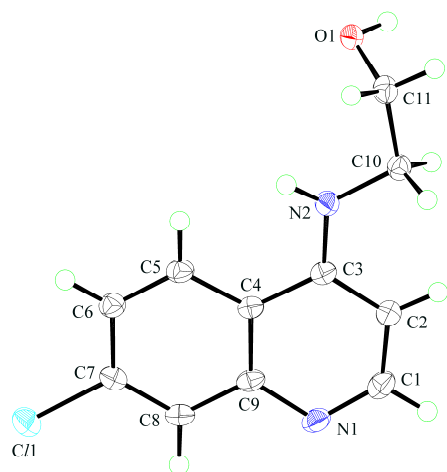


Fig. S12 Molecular structure of (7), showing crystallographic numbering scheme and displacement ellipsoids at the 50% probability level.

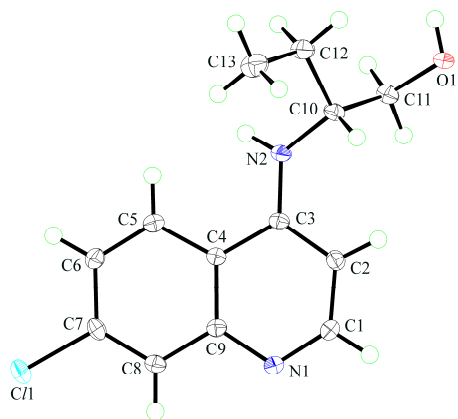


Fig. S13 Molecular structure of **(8)**, showing crystallographic numbering scheme and displacement ellipsoids at the 70% probability level.

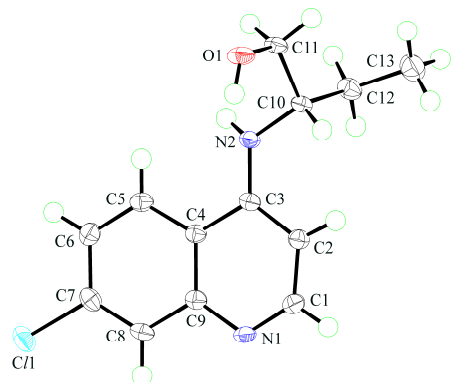


Fig. S14 A side-on view of a layer in **(6)** emphasising the undulating topology. Colour code in this and subsequent diagrams: chloride, cyan; oxygen, red; nitrogen, blue; carbon, grey; and hydrogen, green. For reasons of clarity, only those hydrogen atoms engaged in hydrogen bonding are shown.

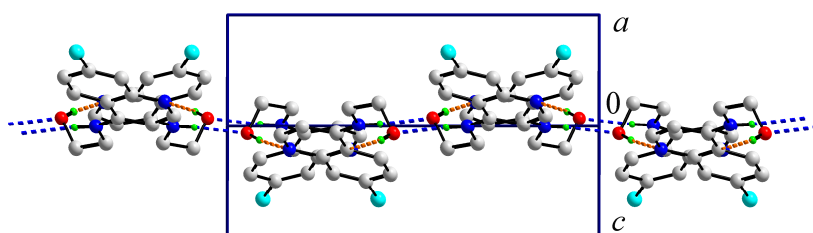


Fig. S15 A side-on view of a layer in **(7)** emphasising the jagged topology.

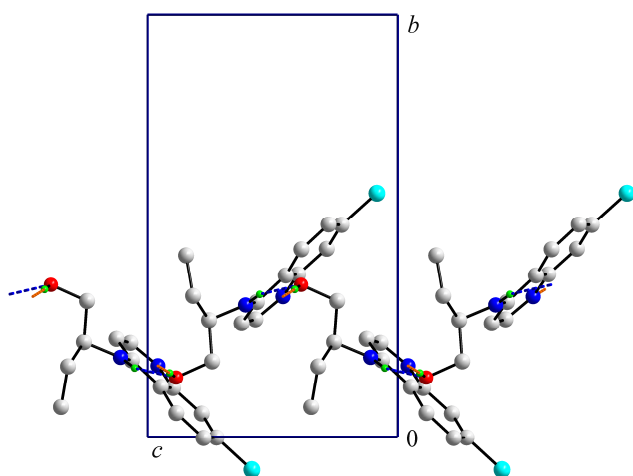
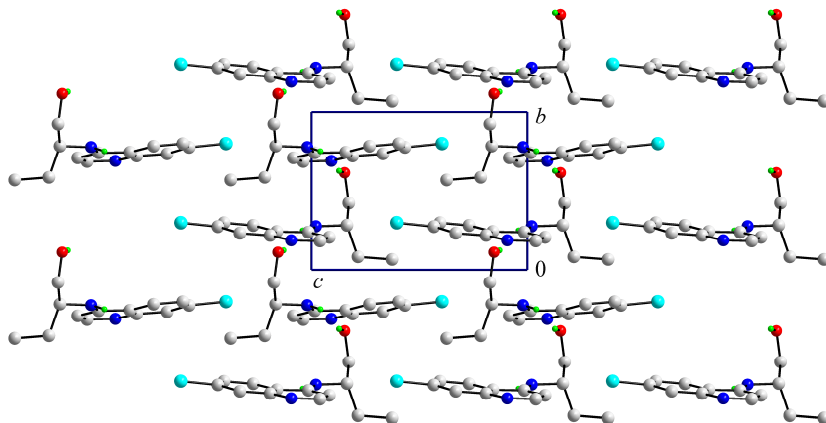


Fig. S16 Views of the crystal packing in (8): projection down the *a*-axis emphasising the inter-digitation of layers.



Characterisation

Characterisation methods

Melting points were determined on a Buchi apparatus and are uncorrected. Infrared spectra were recorded on a Thermo Nicolet Nexus 670 spectrophotometer as KBr pellets and frequencies are expressed in cm^{-1} . Mass spectra (CG/MS) were recorded on an Agilent Technologies 6890/5972A mass spectrometer. NMR spectra were recorded at room temperature on a Bruker Avance 500 spectrometer operating at 500 or 400 MHz (^1H) and 125 or 100 MHz ($^{13}\text{C}\{^1\text{H}\}$), in $\text{Me}_2\text{SO}-d_6$, $\text{MeOH}-d_4$ or $\text{Me}_2\text{CO}-d_6$ solution. Chemical shifts are reported in p.p.m. (δ) relative to TMS. TLC plates coated with silica gel, were run in ethyl acetate and spots were detected by UV light. Microanalytical data were obtained using a Perkin Elmer PE2400 CHN Elemental Analyzer.

7-Chloro-*N*-methyl-4-quinolinamine (**1**), recrystallised from EtOH. Yield: 80%. Obs. (Calc.): C, 62.54 (62.34); H, 4.62 (4.71); N, 14.39 (14.53 %). NMR (400 MHz, $\text{MeOH}-d_4$) ^1H δ : 8.36 (1H, d, $J = 5.6$ Hz, H_2), 8.00 (1H, d, $J = 9.2$ Hz, H_5), 7.77 (1H, d, $J = 2.0$ Hz, H_8), 7.37 (1H, dd, $J = 9.2$ & 2.0 Hz, H_6), 6.45 (1H, d, $J = 5.6$ Hz, H_3), 2.99 p.p.m. (3H, s, Me); ^{13}C δ : 153.8, 152.6, 149.6, 136.4, 127.7, 126.1, 124.3, 118.9, 99.4, 29.9 p.p.m. LC/MS: $m/z[\text{M} + 1]^+$: 193. M. pt. 240 – 242 °C; lit. (T. J. Egan, R. Hunter, C. H. Kaschula, H. M. Marques, A. Mispilon and J. Walden, *J. Med. Chem.*, 2000, **43**, 283) M.pt. 245 °C (sublimes).

7-Chloro-*N*-propyl-4-quinolinamine (**2**), recrystallised from EtOH. Yield: 65%. Obs. (Calc.): C, 65.38 (65.30); H, 5.79 (5.93); N, 12.74 (12.69 %). NMR (500 MHz, $\text{MeOH}-d_4$) ^1H δ 8.32 (1H, d, $J = 6.0$ Hz, H_2), 8.08 (1H, d, $J = 9.0$ Hz, H_5), 7.76 (1H, d, $J = 2.0$ Hz, H_8), 7.36 (1H, dd, $J = 9.0$ & 2.0 Hz, H_6), 6.47 (1H, d, $J = 6.0$ Hz, H_3), 3.32-3.28 (2H, m, NCH_2), 1.76 (2H, sextet., $J = 7.5$ Hz, $\text{CH}_2\text{CH}_2\text{Me}$), 1.04 p.p.m. (3H, t, $J = 7.5$ Hz, Me); ^{13}C δ : 152.8, 152.3, 149.7, 136.3, 128.8, 125.9, 124.3, 118.8, 99.6, 45.8, 22.6, 11.9 p.p.m. LC/MS: $m/z[\text{M}]^+$: 220. M. pt. 144 – 147 °C; lit. (J. Bolte, C. Demuyne and J. Lhomme, *J. Med. Chem.*, 1976, **20**, 106) M. pt. 148 – 148.5 °C.

N-Butyl-7-chloro-quinolinamine (**3**), recrystallised from EtOH. Yield: 75%. Obs. (Calc.): C, 66.39 (66.52); H, 6.53 (6.44); N, 12.01 (11.93 %). NMR (500 MHz, MeOH- d_4) ^1H δ : 8.33 (1H, d, $J = 5.5$ Hz, H₂), 8.08 (1H, d, $J = 9.0$ Hz, H₅), 7.76 (1H, d, $J = 2.0$ Hz, H₈), 7.37 (1H, dd, $J = 9.0$ & 2.0 Hz, H₆), 6.48 (1H, d, $J = 5.5$ Hz, H₃), 3.35-3.31 (2H, m, NCH₂), 1.72 (2H, qnt, $J = 7.5$ Hz, NCH₂CH₂), 1.48 (2H, sextet, $J = 7.5$ Hz, CH₂Me), 1.00 p.p.m. (3H, t, $J = 7.0$ Hz, Me); ^{13}C δ : 152.8, 152.4, 149.7, 136.3, 127.6, 125.9, 124.3, 118.8, 99.6, 43.8, 31.6, 21.4, 14.2 p.p.m. LC/MS: $m/z[M]^+$: 234. M. pt. 132 – 135 °C; lit. (C. N. M. Bakker, *J. Lab. Comp. Radiopharm.*, 1978, **15**, 681) M. pt. 130 – 132 °C.

N-(2-Chloroethyl)-*N*-(7-chloro-4-quinolinyl)amine (**4**), recrystallised from MeOH. Yield: 93%. Obs. (Calc.): C, 57.35 (57.18); H, 4.52 (4.36); N, 12.42 (12.12 %). NMR (500 MHz, Me₂CO- d_6) ^1H δ : 8.49 (1H, d, $J = 5.0$ Hz, H₂), 8.16 (1H, d, $J = 9.0$ Hz, H₅), 7.86 (1H, d, $J = 2.0$ Hz, H₈), 7.41 (1H, dd, $J = 9.0$ and 2.0 Hz, H₆), 6.93 (1H, s, NH), 6.63 (1H, t, $J = 5.0$ Hz, H₃), 3.89 (2H, q, $J = 6.0$ Hz, NCH₂), 3.81 p.p.m. (2H, t, $J = 6.0$ Hz, CH₂Cl); NMR (DMSO- d_6) ^{13}C δ : 153.0, 150.7, 150.6, 134.9, 129.3, 125.6, 123.8, 118.6, 100.0, 45.5, 42.9 p.p.m. M. pt. 131 °C.

N-(2-Azidoethyl)-7-chloro-quinolinylamine (**5**), recrystallised from EtOH. Yield: 46%. Obs. (Calc.): C, 53.20 (53.47); H, 4.22 (4.08); N, 27.95 (28.33 %). NMR (500 MHz, Me₂CO- d_6) ^1H δ : 8.49 (1H, d, $J = 5.0$ Hz, H₂), 8.17 (1H, d, $J = 9.0$ Hz, H₅), 7.85 (1H, d, $J = 2.0$ Hz, H₈), 7.40 (1H, dd, $J = 9.0$ & 2.0 Hz, H₆), 6.89 (1H, s, NH), 6.64 (1H, d, $J = 5.5$ Hz, H₃), 3.72-3.62 p.p.m. (4H, m, CH₂CH₂); NMR (DMSO- d_6) ^{13}C δ : 153.0, 150.5, 150.7, 134.9, 129.2, 125.5, 123.9, 118.7, 100.0, 50.4, 43.2 p.p.m. LC/MS: $m/z[M - 1]$: 246. M. pt. 145 – 148 °C.

2-[(7-Chloro-4-quinolinyl)amino]ethanol (**6**), recrystallised from EtOH. Yield: 93%. Obs. (Calc.): C, 59.21 (59.33); H, 5.17 (4.98); N, 12.74 (12.57 %). NMR (400 MHz, DMSO- d_6) ^1H δ : 8.38 (1H, d, $J = 5.4$ Hz, H₂), 8.26 (1H, d, $J = 9.0$ Hz, H₅), 7.78 (1H, d, $J = 2.1$ Hz, H₈), 7.56 (1H, dd, $J = 9.0$ & 2.1 Hz, H₆), 7.25 (1H, t, $J = 5.0$ Hz, NH), 6.49 (1H, d, $J = 5.4$ Hz, H₃), 4.84 (1H, t, $J = 5.5$ Hz, OH), 3.66 (2H, q, $J = 5.9$ Hz) & 3.35 p.p.m. (2H, q, $J = 5.9$ Hz, CH₂CH₂); ^{13}C δ : 151.8, 150.2, 149.1, 133.3, 127.5, 124.0, 124.0, 117.4, 98.7, 58.8, 45.1 p.p.m. LC/MS: $m/z[M + 1]$: 223. M. pt. 212 – 214 °C, lit. (T. J. Egan, R.

Hunter, C. H. Kaschula, H. M. Marques, A. Misplon and J. Walden, *J. Med. Chem.*, 2000, **43**, 283) 217 – 219 °C.

2-[(7-Chloro-4-quinolinyl)amino]-1-butanol (**7**), recrystallised from MeOH. Yield: 75%. Obs. (Calc.): C, 62.45 (62.27); H, 6.11 (6.03); N, 10.97 (11.17 %). NMR (400 MHz, MeOH- d_4) ^1H δ : 8.33 (1H, d, $J = 5.6$ Hz, H₂), 8.18 (1H, d, $J = 8.8$ Hz, H₅), 7.77 (1H, d, $J = 2.0$ Hz, H₈), 7.38 (1H, dd, $J = 8.8$ & 2.0 Hz, H₆), 6.59 (1H, d, $J = 5.6$ Hz, H₃), 3.74-3.69 (2H, m, NCH₂ & CH₂OH), 1.88-1.66 (2H, m, CH₂Me), 1.02 p.p.m. (3H, t, $J = 7.6$ Hz, Me); ^{13}C δ : 153.0, 152.4, 149.9, 136.5, 127.6, 126.1, 124.5, 118.9, 100.2, 64.4, 57.6, 25.2, 11.1. LC/MS: m/z[M - 1]: 249. M .pt. 150 °C.

(2*S*)-2-[(7-Chloro-4-quinolinyl)amino]-1-butanol (**8**), recrystallised from Me₂CO. Yield: 70%. Obs. (Calc.): C, 62.14 (62.27); H, 6.20 (6.03); N, 11.31 (11.17 %). NMR (500 MHz, MeOH- d_4) ^1H δ : 8.33 (1H, d, $J = 5.5$ Hz, H₂), 8.20 (1H, d, $J = 9.2$ Hz, H₅), 7.77 (1H, d, $J = 2.0$ Hz, H₈), 7.41 (1H, dd, $J = 9.2$ & 2.0 Hz, H₆), 6.62 (1H, d, $J = 5.5$ Hz, H₃), 3.72-3.68 (2H, m, NCH₂ & CH₂OH), 1.88-1.66 (2H, m, CH₂Me), 1.02 p.p.m. (3H, t, $J = 7.5$ Hz, Me); ^{13}C δ : 153.1, 152.2, 149.7, 136.7, 127.5, 126.1, 124.6, 119.0, 100.2, 64.4, 57.5, 25.2, 11.1 p.p.m. LC/MS: m/z[M - 1]: 249. M .pt. 197 – 199 °C.